EARTH SURFACE PROCESSES AND LANDFORMS
Earth Surf. Process. Landforms (2018)

Published online in Wiley Online Library
(wileyonlinelibrary.com) DOI: 10.1002/esp.4462

Quantification of cliff retreat in coastal Quaternary sediments using anatomical changes in exposed tree roots

Jérôme Lopez-Saez,[1]* Christophe Corona,[2] Pauline Morel,[3] Georges Rovéra,[4] Thomas J.B. Dewez,[5] Markus Stoffel[1] and Frédéric Berger[3]
[1] Institute for Environmental Sciences, Climate Change Impacts and Risks in the Anthropocene (C-CIA), University of Geneva, Geneva, Switzerland
[2] Centre National de la Recherche Scientifique (CNRS), UMR 6042, GEOLAB, Clermont-Ferrand, Cedex France
[3] Irstea, UR LESSEM, Université Grenoble Alpes, St-Martin-d'Hères, France
[4] CNRS, UMR 5194 PACTE Territoires, Grenoble, France
[5] Risk and Prevention Direction BRGM, Orléans 45060 and PACA Territorial Direction, Marseille, France

Received 29 November 2016; Revised 14 June 2018; Accepted 20 June 2018

*Correspondence to: Jérôme Lopez-Saez, Institute for Environmental Sciences, Climate Change Impacts and Risks in the Anthropocene (C-CIA), University of Geneva, 66 Boulevard Carl-Vogt, CH-1205 Geneva, Switzerland. E-mail: jerome.lopez-saez@unige.ch

ESPL
Earth Surface Processes and Landforms

ABSTRACT: Sea cliffs represent 80% of the world's coasts and can be found virtually in all types of morphogenetic environments. Most studies on rocky environments focused on the impacts of modern sea level rise on cliff stability derived from sequential surveys, direct measurements or erosional features in anthropogenic structures. In this study, we explore the potential of dendrogeomorphic techniques to quantify multidecadal changes in coastal environments on Porquerolles Island (France). We sampled a total of 56 cross-sections from 16 *Pinus halepensis* Mill. roots growing on former alluvial deposits and on sandy-gravelly cliffs to quantify mean annual cliff retreat rates as well as changes in cliff geometry. Anatomical changes in roots have been used successfully in the past to quantify continuous denudation rates on slopes, channel incision and gullying processes but the approach has not been used so far in a coastal cliff context. At Porquerolles Island, reconstructed rates of cliff retreat cover 30–40 years and show average erosion rates between 0.6 and 3.9 cm yr^{-1} (average: 2.1 cm yr^{-1}). Highest rates are observed at Pointe de la Tufière (2.6–3.9 cm yr^{-1}), a small rock promontory that is more exposed to wave and storm surges than the remainder of the study area. By contrast, lower erosion rates are recorded at cliffs protected by the La Courtade pocket beach (0.6–1.9 cm yr^{-1}). This contribution demonstrates that dendrogeomorphic analyses of roots clearly have a significant potential and that they are a powerful tool for the quantification of multidecadal rates of cliff retreat in areas where measurements of past erosion are lacking. More specifically, the approach also has clear advantages over the shorter time series obtained with repeat monitoring (e.g. terrestrial laser scanning, sensors, erosion pins) or over longer, but more coarsely resolved records obtained from aerial photographs or radio-nuclides. © 2018 John Wiley & Sons, Ltd.

KEYWORDS: tree-ring; erosion rates; coastal cliffs; Porquerolles; cliff retreat

Introduction

Sea cliffs comprise 80% of the world's coasts (Granja, 2009), along which almost one-fourth of the global population resides (Small and Nicholls, 2003; Young *et al.*, 2009a). Coastal changes and erosion therefore can induce a threat for human activity and safety. Indeed, seacliff erosion not only threatens coastal structures, but may also negatively affect public property, recreational resources, public safety, and major transportation corridors. As a result of the predicted acceleration of coastal erosion due to climatic changes and the related sea-level rise (Zhang *et al.*, 2004; Hurst *et al.*, 2016, Naylor *et al.*, 2017), cliff retreat has been the subject of a wealth of studies which mostly aimed at the quantification of erosional phenomena and their timescales (Katz and Mushkin, 2013; Trenhaile, 2014; see Table I for a recent review). Conventional techniques used to quantify cliff retreat include erosion pins installed at the base of rock masses, repeat aerial photography, comparison of different generations of topographic maps, or *in situ* surveys (Lim *et al.*, 2005; Brooks and Spencer, 2010; Dornbusch *et al.*, 2008). More recently, cosmogenic radionuclides as well as LiDAR (light detection and ranging) and stereophotogrammetric surveys have been used (i) to date and/or quantify changes in the coastal zone and (ii) to demonstrate their huge potential to monitor and model cliff erosion (e.g. Young *et al.*, 2009a; Lim *et al.*, 2010; Regard *et al.*, 2012; Earlie *et al.*, 2015a, 2015b; Hurst *et al.*, 2016). As a result of the great monitoring efforts required, observational time series of long-term erosion cliff retreat remain exceptional, and thereby prevent the creation of reliable data on average cliff retreat at larger (decadal to

Table I. Overview of work published on coastal cliff retreat. Identifiers are the same as in Figure 7

Index Author(s), Year	Journals	Country	Latitude (deg)	Longitude (deg)	Location	Lithology	Erosion rate (m yr^{-1})	Methods	Period
1 Agar, 1960	Proceedings	UK	54.6	−1.06	North Yorkshire	Mudstone, sandstone	0.03	Photogrammetry	1892–1960
2 Andriani and Walsh, 2007	Geomorphology	Italy	41	17.2	Apullia	Biocalcarenites	0.2	Photogrammetry	1930–2003
3 Borges, 2003	PhD Thesis	Portugal	37.8	−25.5	Azore archipelago	Rocky coast	0.05	NA	NA
4 Brooks and Spencer, 2010	Geomorphology	UK	52.37	1.7	Suffolk	Softrock	0.9–3.5	Historic maps	1983–2003
5 Brooks *et al.*, 2012	Geomorphology	UK	52.3	1.68	Suffolk	Softrock	3.5	Photogrammetry	1883–2010
6 Brooks *et al.*, 2016	Earth Surface Processes and Landforms	UK	52.95	0.81	Norfolk	mud- and sand-flats	1.15	Aerial photograph	1891–2013
7 Lopez-Saez *et al.*, this study	Earth Surface Processes and Landforms	France	43.01	6.3	Porquerolles	Sandstone	0.021	Exposed roots	1976–2011
8 Costa *et al.*, 2004	Engineering Geology	France	50.1	1.45	Normandy	Chalk	0.3	NA	1966–1995
9 Dornbusch *et al.*, 2008	Marine Geology	UK	50.76	0.11	Sussex	Chalk	0.35	Photogrammetry	1873–2001
10 Earlie *et al.*, 2015a	Journal of Coastal Conservation	UK	50.15	5.03	Cornwall	Softrock	<0.1–0.5	LiDAR	2007–2011
11 Earlie *et al.*, 2015b	Geophysical Research Letter	UK	50.05	5.18	Cornwall	Softrock	0.09	LiDAR	2007–2011
12 Greenwood and Orford, 2007	Geomorphology	UK	54.48	−5.58	Strangford Lough	Glacigenic sediments	0.08	Erosion pines	1994–1997
13 Hall *et al.*, 2002	Coastal Engineering	UK	50.88	0.68	Sussex	Softrock	0.47	Historic maps	1907–1991
14 Hapke and Green, 2004	USGS	USA	37	−122	California	Various	0.12–0.25	Various	Various
15 Harper, 1978	Arctic	USA	71.3	−156.8	Alaska	Silts and sands	0.3	Photogrammetry	1949–1976
16 Henaff *et al.*, 2002	Géomorphologie	France	49.7	0.2	Pays de Caux	Chalk	0.06	Photogrammetry	1824–1986
17 Kumar *et al.*, 2009	Environmental Geology	India	10.76	75.91	Kerala	Sandstone, clay and silt	0.5	GPS survey	2004–2006
18 Lee, 2008	Geomorphology	UK	52.93	1.3	Norfolk	Sand and clay	1.05	GPS survey	1992–2003
19 Lim *et al.*, 2009	Journal of Coastal Research	South Korea	35.5	126.25	Hampyung Bay	Soft soil	1.4	Aerial photograph	1976–1990
20 Marques, 2003	Proceedings	Morocco	35.2	−6.15	Larache	Sandstone	0.08	Photogrammetry	1961–1997
21 Marques, 1997	PhD Thesis	Portugal	37.01	−8.01	Algarve	Sandstone	0.019	Photogrammetry	1947–1991
23 Moon and Healy, 1994	Journal of Coastal Research	New Zealand	−36.8	174.75	Auckland	Sandstone and silstone	0.04	Dated structures	NA
24 Moore and Griggs, 2002	Marine Geology	USA	36.97	−122.03	California	Sandstone and silstone	0.15	Photogrammetry	1953–1994
25 Orviku *et al.*, 2013	Journal of Coastal Research	Estonia	59.45	24.53	Kakumae	Sandstone	0.6	Field survey	1996–2006
26 Pierre, 2006	Geomorphology	France	50.8	1.58	Boulonnais	Clay and sandstone	0.08	Photogrammetry	1939–2003
27 Poulton *et al.*, 2006	Bulletin of the Geological Society of Norfolk	UK	52.49	1.31	Norfolk	Softrock	8.75	Various	1992–2004
29 Rudberg, 1967	Geografiska annaler	Sweden	57.4	18.8	Gotland	Limestone and marl	0.05	Photogrammetry	1899–1955
30 Stephensen *et al.*, 2012	Marine Geology	Australia	−38.32	143.58	Victoria	Sandstone and mudstone	0.00031	Field survey	1979–2011
32 Wangensteen *et al.*, 2007	Polar Research	Norway	78.26	21.95	Svalbard	Dolomit limestone	0.003	Photogrammetry	2002–2004
33 Xeidakis *et al.*, 2007	Environmental Geology	Greece	40.84	25.87	Alexandroupolis	Sandy-silty sediments	0.5	Photogrammetry	NA
34 Young and Ahsford, 2006	Journal of Coastal Research	USA	33.12	−117.19	California	Mudstone and sandstone	0.08	LiDAR	1998–2004
35 Young *et al.*, 2009a	Geomorphology	USA	36.96	−121.98	California	Sand and clay	0.3	LiDAR	2002–2006
36 Zviely and Klein, 2004	Earth Surface Processes and Landforms	Israel	32.38	34.86	Beit–Yannay	Quartzose	0.2	Photogrammetry	1918–2000

centennial) temporal scales. Other indirect methods might thus be needed to assess longer term process activity and the correlation and interdependence of the latter with environmental changes. In this paper the dendrogeomorphic analysis (Alestalo, 1971; Stoffel and Bollschweiler, 2008; Stoffel *et al.*, 2010) of exposed tree roots and the interpretation of anomalies registered in their growth rings are used as an alternative to the methods traditionally used to quantify cliff recession.

Dendrogeomorphology is typically used at locations where geomorphic process activity interferes in space and time with vegetation (Stoffel and Bollschweiler, 2008; Stoffel *et al.*, 2010). The approach, first elucidated by Alestalo (1971), takes advantage of the fact that trees growing in temperate climates do not only form yearly increment rings but that they will also record the occurrence of external disturbances in their growth-ring record, thus allowing accurate dating and reconstruction of past process histories (Stoffel and Corona, 2014). Previous dendrogeomorphic work focused primarily on tree stem and only to a lesser extent on tree roots. In addition, research on roots was mostly centered on the sprouting of adventitious roots to infer sediment deposition during floods (Martens, 1993; Nakamura *et al.*, 1995) or debris flows (Strunk, 1989, 1991, 1997). Another focus was on the determination of aerial erosion rates over timescales of hundreds to thousands of years, based on the ratio between the minimum depth of erosion – obtained from the reconstructed root diameter at the moment of denudation – and the time (i.e. number of growth rings) passed since root exposure (Eardley and Viavant, 1967; LaMarche, 1968; Gärtner, 2001; McAuliffe *et al.*, 2006). More recently, microscopic approaches have been used to determine the year of exposure. These approaches focus on changes in the anatomical structure of tracheids in conifer roots (Corona *et al.*, 2011b; see Stoffel *et al.*, 2013, for a detailed review). The approach has been used in various environments, but mostly in relation with gullying processes (Vandekerckhove, 2001; Malik, 2008; Ballesteros-Cánovas *et al.*, 2017), aerial (or sheet) (Bodoque *et al.*, 2005; Lopez Saez *et al.*, 2011; Lucía *et al.*, 2011), river bank (Malik, 2006; Hitz *et al.*, 2008a; Stoffel *et al.*, 2012), or lake shore (Fantucci, 2007) erosion (see Table II for an overview).

In this contribution, we aim at testing the potential of wood-anatomical signatures in tree roots to quantify spatial and temporal changes in cliff retreat in a marine context and at vertical sites for which roots have not been employed in the past. We document erosion signals and rates of erosion for 56 cross-sections selected from *Pinus halepensis* Mill. roots from sandy-gravelly cliffs and compare results with rates found in the literature and for sites located next to our study region on Porquerolles Island.

Study Site

Porquerolles Island (Var, France) is located in the Mediterranean Sea, east-southeast (E-SE) of Toulon; the island belongs to the Hyères Islands, which are partially closing the natural Hyères harbor (Figure 1A). Porquerolles Island is 7.5 km long, 1.7 km wide, reaches 142 m above sea level (a.s.l.), and has a surface of 12.54 km^2. The south (S) and southwest (SW) coasts of Porquerolles are lined with cliffs, whereas the north (N) and northwest (NW) coasts exhibit an alternation of small capes (Pointe de Lequin, Pointe Bon-Renaud) and beaches, with the latter being located predominantly at the mouth of floodplains (Notre-Dame, La Courtade, Plage d'Argent).

Some parts of the coastline display small cliffs (up to 5 m in height) composed of sands and gravels, laid behind beaches and next to capes. In this study we focused on such cliffs located in the area of La Courtade (43°003 N; 6°213 E; Figure 1C). The island has a geological structure very similar to that of the Maures massif (Bordet *et al.*, 1976); it consists predominantly of phyllitic rocks (Figure 1C) which alternate with quartzite veins. The most important units form a large N–S ridge and extend from Cape des Medes to Mont-Sarranier (126 m). The cliffs investigated here are dark and light ocher in color and consist of a consolidated sandy-gravelly matrix of paleo-alluvial origin (Würmian age, Bordet *et al.*, 1976). The base of the cliffs (Figures 2A and 2B) consists of compact sands (stratum 1) covered with torrential strata revealing angular, decimetric (stratum 2) to centimetric (stratum 3) phyllite and quartzite debris of periglacial origin. The uppermost layer of the cliff is formed by sand and gravel horizons (stratum 4). The deposits under investigation have been affected by sea erosion throughout the Holocene to form receding cliffs located behind pocket beaches (Figures 1D and 1E). As described by Lee (2008), cliff recession is characterized by the balance between the strength of cliff materials and the stresses imposed on the cliff by gravity and the kinetic energy of waves at the cliff foot. Albeit slope processes dominate recession rates in sheltered inlets and bays (e.g. Greenwood and Orford, 2007), most of the time geological materials and wave attack are the dominant factors leading to open-coast recessions processes (Sunamura, 1992; Costa *et al.*, 2004; Lee, 2008). Present-day erosion processes are driven by ongoing sea-level rise and themechanical erosion of the cliffs (e.g. swell in particular) as well as by subaerial processes. Observations also point to the importance of Mistral winds (blowing from NW, after the passage of low-pressure systems in the Gulf of Genoa) on wave action and thus on erosion processes (Gervais, 2012) (Figure 1B). This wind system also leads to storm surges and the hydration of cliffs. The short foreshore (5–10 m) and the small difference in height between the average level of the water and the bottom of the cliffs (0.5–1 m) allow waves and swells to directly impact the foot of the cliffs. Some notches are thus carved up to 1 m in height and at depths of several decimeters (Figures 1D and 1E.). These sporadic episodes of storm-related erosion are complemented by surficial and quasi-continuous rill erosion, with the latter being driven by seasonal variations in weather and the rhythmicity of splash, desiccation–hydration alternations, or salt weathering.

Material and Methods

Methods of cliff retreat reconstruction

For a precise quantification of the cliff retreat based on root exposure, two parameters are needed: the number of annual rings since exposure (NRex) and the thickness of the eroded soil layer (Er). When a root loses its soil cover, a series of anatomical changes (cell size, tangential growth, compression wood) will occur in terms of ring growth, firstly because of the effect of the exposure itself (e.g. variations in edaphic temperature and humidity, reduction in soil cover pressure), but also because of mechanical stress (e.g. abrasion) that a root will undergo when exposed. As proposed by Corona *et al.* (2011b), a reduction of cell lumen area in earlywood tracheids by about 50% can be used as a distinct sign of exposure in conifer roots (Figure 3). To calculate the annual erosion rate Era, Er is divided by the number of rings formed since the year of exposure (NRex):

$$\mathrm{Era} = \mathrm{Er}/\mathrm{Nrex} \quad (1)$$

Table II. Overview of published reconstructions of erosion using dendrogeomorphic techniques

Process	Environment	Location	Latitude	Longitude	Rates (mm yr^{-1})	Number of roots	Number of samples	References
Bank erosion	Riverbank	Patagonia	40°56′ S	71°24′ W	—	31	64	Stoffel *et al.*, 2012
Bank erosion	Riverbank	Czech Republic	50°15′ N	15°05′ E	—	23	60	Malik and Matyja, 2008
Bank erosion	Riverbank	Switzerland & Germany	46°17′ N	7°32′ E	—	18	38	Gärtner *et al.*, 2001
Gully retreat	Gullies	Czech Republic	49°22′ N	18°7′ E	150–3000	21	21	Silhan, 2012
Gully retreat	Gullies	Poland	50°21′ N	17°51′ E	0.63	28	53	Malik, 2008
Sheet erosion	Gullies	Spain	41°10′ N	3°48′ W	6.2	21	21	Bodoque *et al.*, 2015
Sheet erosion	Hillslopes	China	36°69′ N	102°71′ E	3.3–13.5	23	40	Zhou *et al.*, 2013
Sheet erosion	Hillslopes	Iran	—	—	0.54	42	42	Bahrami *et al.*, 2011
Sheet erosion	Badlands	Spain	41°10′ N	3°48′ W	6.2–8.8	29	29	Bodoque *et al.*, 2011
Sheet erosion	Gullies	France	44°08′ N	6°20′ E	5.9–6.2	17	39	Corona *et al.*, 2011a
Sheet erosion	Gullies	France	44°08′ N	6°20′ E	5.9	27	48	Lopez-Saez *et al.*, 2011
Sheet erosion	Hiking trails	Spain	40°59′ N	4°05′ E	—	18	18	Rubiales *et al.*, 2008
Sheet erosion	Forest	Spain	40°12′ N	3°34′ W	3.5–8.8	49	49	Pérez-Rodriguez *et al.*, 2007
Sheet erosion	Hillslopes	USA	36°09′ N	109°33′ W	2.0–3.0	—	—	Wawrzyniec *et al.*, 2007
Sheet erosion	Hillslopes	USA	36°09′ N	109°33′ W	1.9	49	49	Scuderi *et al.*, 2008
Sheet erosion	Hiking trails	Spain	40°52′ N	4°01′ W	1.6–2.6	86	86	Bodoque *et al.*, 2005
Sheet erosion	Various	USA	39°20′ N	106°52′ W	1.18	20	83	Carrara and Carroll, 1979
Shore erosion	Lakes	USA	32°23′ N	110°42′ W	1	—	—	Danzer, 1996
Soil erosion	Badlands	France	44°08′ N	6°20′ E	0.5	23	123	Corona *et al.*, 2011b
Soil erosion	Karst area	China	14°26′ N	105°42′ E	—	24	24	Luo *et al.*, 2011
Soil erosion	Rangelands	Patagonia	42°58′ S	64°20′ W	2.4–3.2	15	15	Chartier *et al.*, 2009
Soil erosion	Gullies	Poland	50°04′ N	14°24′ E	—	28	53	Malik, 2006
Soil erosion	Hiking trails	Italy	46°24′ N	10°31′ E	2.7	72	72	Pelfini and Santilli, 2006
Soil erosion	Roadcut	USA	—	—	10.0–11.0	41	41	Megahan *et al.*, 1983
Soil erosion	Rangelands	Kenya	1°26′ S	36°57′ E	5.5	14	14	Dunne *et al.*, 1978
Bank erosion	Riverbank	USA	78°51′ N	38°7′ W	3.85	73	73	Stotts *et al.*, 2014
Sheet erosion	Gullies	Spain	41°9′ N	3°48′ W	4.4–8.8	46	46	Ballesteros-Cánovas *et al.*, 2015
Soil erosion	Karst area	China	—	—	—	11	22	Mei *et al.*, 2015
Soil erosion	Methodological contribution	NA	—	—	—	—	—	Ballesteros-Cánovas *et al.*, 2013
Soil erosion	NA	China	25°41′ N	101°49′ E	1.04–3.61	25	136	Sun *et al.*, 2014
Bank erosion	Riverbank	USA	—	—	1–259	46	78	Dick *et al.*, 2013
Soil erosion	Rills and gullies	Argentina	31°34′ S	64°50′ W	—	14	14	Chartier *et al.*, 2016
Coastal erosion	See shore	France	43°00′ N	6°21′ E	21	17	56	Present study

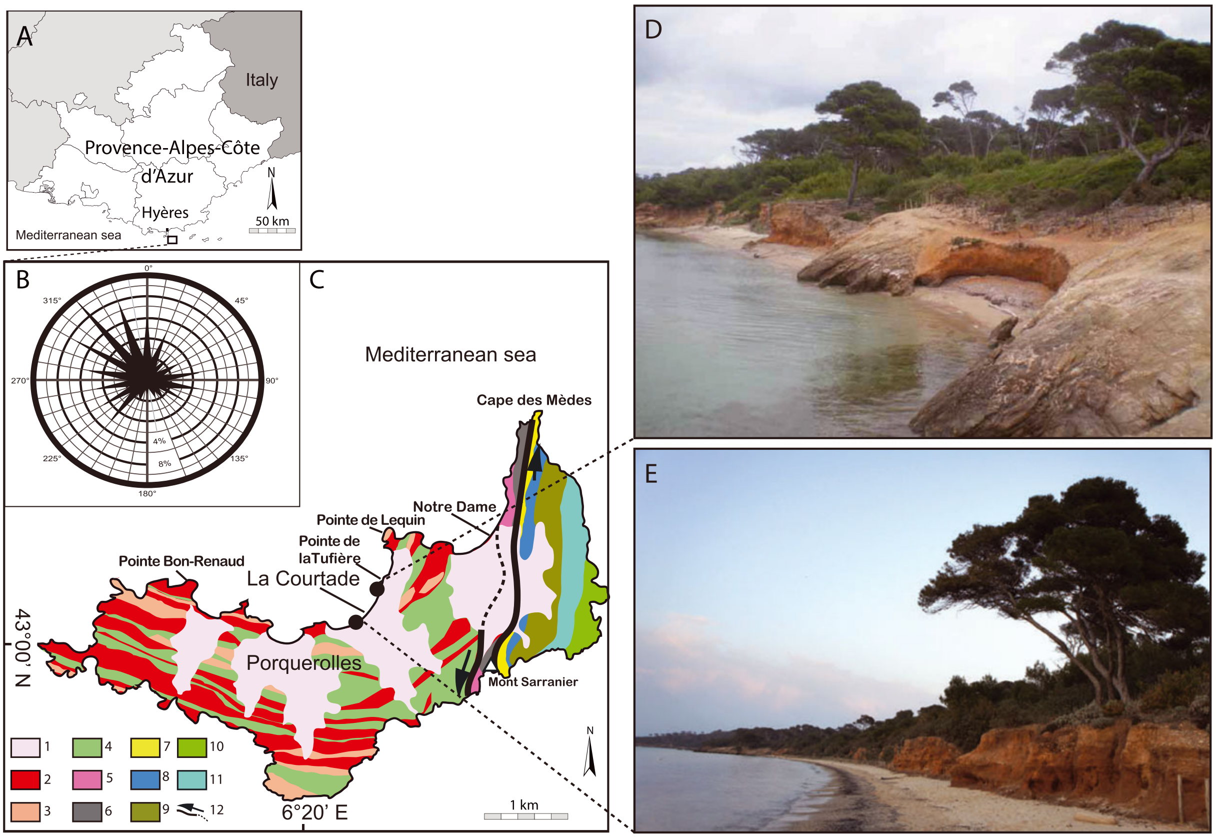

Figure 1. (A) Location of the study site; (B) compass showing the main wind directions over Porquerolles; (C) simplified geological map of Porquerolles Island adapted from Bellot (2004): 1. Fluvial deposit, 2. Succesion of sandstone/schist, 3. Sandstone, 4. Schist, 5. Succesion of finely conglomeratic sandstone/banded schist interleaved with limestone 6. Finequartzite, 7. Yellow quartzitesfrom Cap des Mèdes, 8. Schists/ micaschists, 9. Black- green-schists, quartzites, sandstone, 10. Monotonous green schists, 11. Schist interleaved with metabasit and calcschist, 12. Ductile srtike-slip fault (potential and observed); (D) the northern part of La Courtade beach is characterized by an alternation of rocky headlands (phyllite) as well as (E) by pocket beaches dominated by sandy-gravelly cliffs affected by erosion. [Colour figure can be viewed at wileyonlinelibrary.com]

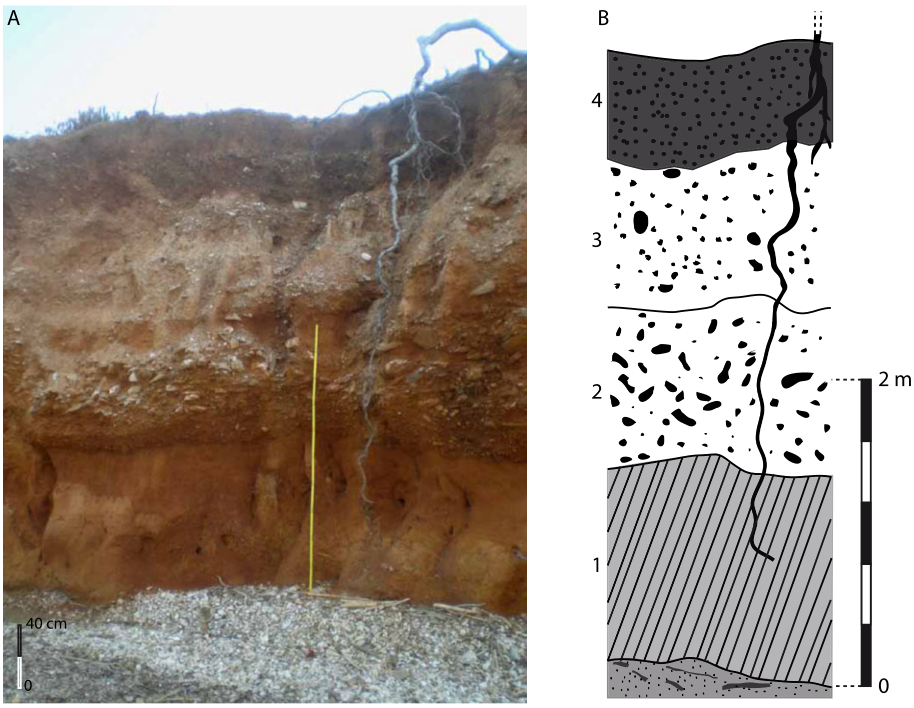

Figure 2. (A) Segment of a sandy-gravelly cliff close to the Pointe de la Tufière. (B) The base of the landform corresponds to (1) a compact sandy stratum and a torrential deposit revealing decimetric (2) to centimetric (3) angular phyllite and quartzite debris. The upper part is made of (4) sand and gravel horizons, sometimes individual, sometimes overlapping. Cliff retreat is revealed by the exposure of a *Pinus halepensis* Mill. root. [Colour figure can be viewed at wileyonlinelibrary.com]

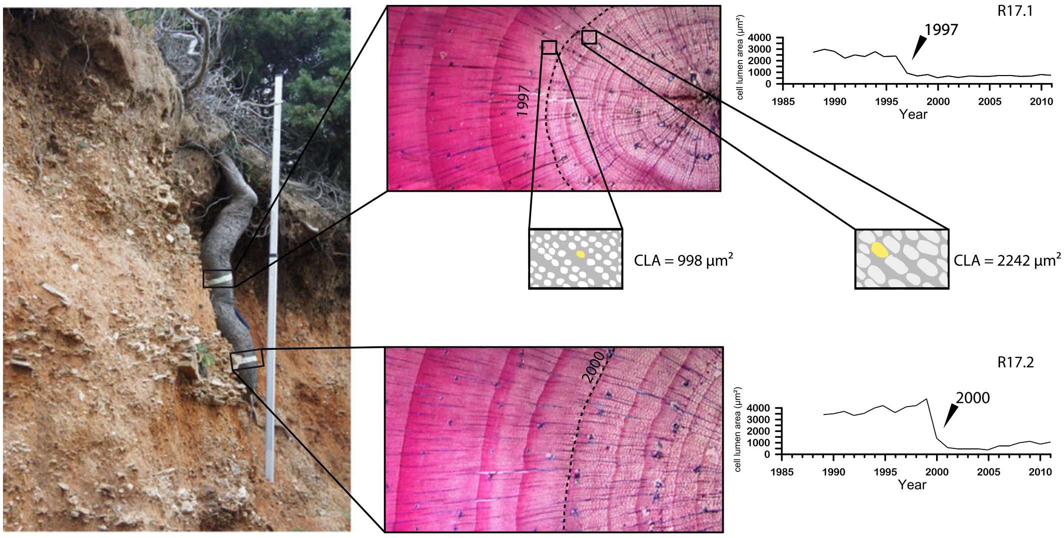

Figure 3. Micro-sections of roots R17.1 and R17.2 with exposure signals in 1997 and 2000, respectively. Determination of exposure years was based on the sharp decrease of cell lumen area of earlywood tracheids. [Colour figure can be viewed at wileyonlinelibrary.com]

Sampling strategy and root-ring analysis

At the study site, 56 root cross-sections (six from buried and 50 from exposed roots) were sampled from 16 different roots of 16 *P. halepensis* Mill. trees, and at a minimum distance of 50 cm from the stem basis. This distance has been chosen as (i) stem movement induced by ongoing growth tends to pull roots upwards (Stokes and Berthier, 2000), and as (ii) roots close to the stem basis and growing near the soil surface often experience bending stress resulting from stem displacement (Watson, 2000), and therefore exhibit asymmetric growth structures in cross-sections. The position of exposed roots with respect to the present cliff surface was documented in detail before the root was actually cut and data recorded on the stratigraphic position, distance of the root section from the tree trunk, aspect, and slope (for a complete description of the method, see Corona *et al.*, 2011b). The horizontal distance between the root and the cliff surface (Er) was determined with a depth gage (accuracy ±1 mm); in cases where the distance between the root and the cliff exceeded 25 cm, a metal ruler (±5 mm) was used instead. Root sample locations were recorded using a Trimble GeoExplorer (with < 1 m accuracy) and roots were then positioned in a geographical information system (GIS; ArcGIS 10.1; Kennedy, 2009) as geo-objects, where erosion rates could be linked as attributes to each single root section.

In the field, the root sampling strategy was defined according to geomorphic units (i.e. rocky point, pocket beach) and to the stratigraphic profile of the cliffs (Figures 2A and 2B). Samples were distributed within the two geomorphic units and the four strata of the stratigraphic profile. In order to determine Nrex, sampled roots were then cut into discs about 2 cm thick and air-dried for ~30 days, before they were prepared for macroscopic analysis (i.e. sanded sequentially with 60, 80, 320, and 600 grit-sanding belts). Ring-width data were obtained on four radii per cross-section using a LINTAB measurement device (Rinn and Jäkel, 1996). Thereafter, we prepared root discs for microscopic analysis. Small cubes were cut from the cross-sections (maximum 2 cm × 4 cm) from which microsections where cut with a Reichert sliding microtome (thickness of cuts ~15 µm). The microsections were treated with sodium hypochlorite (NaOCl) solution, deionized water, and soluble safranin before they were dehydrated with alcohol and xylol (Schweingruber, 1978; Arbellay *et al.*, 2012). The microsections were mounted on slides, embedded in Canada balsam, and dried at 60°C for 24 hours. Microsections were then observed and photographed with a digital imaging system under optical microscopy. Measurement of cell lumen area in earlywood tracheids was performed with the semiautomated WinCELL2005 software. Following Rubiales *et al.* (2008), cell lumen area was determined through an averaging of 12 cell measurements per growth ring. In addition, and in order to detect potential anatomical changes that could occur before root exposure (Corona *et al.*, 2011b) and to assess the maximum depth at which anatomical changes may occur, we compared cell changes in exposed sections with those observed in buried sections embedded into the cliff (−2 to −18 cm, Table III) (Corona *et al.*, 2011b).

Results

Anatomical changes in roots

The innermost rings of the roots sampled were dated to between AD 1976 (R16.4) and 1999 (R4.3), with a mean root age of 22 years and a standard deviation of ±6 years (Table III). The wood anatomical structure of the exposed root sections R17.1 and R17.2, shown in Figure 3 for the years 1988–2011 and 1989–2011, respectively, illustrates anatomical changes that occurred in each section after exposure. Both samples were taken half way up the cliff (strata 2 and 3). These roots show thin cell walls and large cell lumina in earlywood tracheids until 1996 (R17.1) and 1999 (R17.2), respectively. From 1997 (2000) onwards, root rings form thicker-walled tracheids and more stem-like wood structures, with very distinct latewood and cell lumen area reductions > 50% (from 2560 to 982 μm^2, or −62% for R17.1; and from 3600 to 900 μm^2, or −75%, for R17.2, respectively). Similar sudden and sharp relative reductions in cell lumen area as those described earlier are observed for all exposed roots chosen for analysis between 1991 and 2006 (mean: 2000; Table III). Conversely, the buried parts of the roots sampled in this study (i.e. R5.3 to R5.5 and R16.5 to R16.7, located at depth ranging from −2 to −18 cm within the strata) are characterized by large tracheids with thin and poorly lignified cell walls as typical for buried roots.

Heights of the exposed parts of the 50 cross-sections of roots – as measured in the field (Er) – varied from 2 to 87 cm (mean: 30.4 cm), representing an overall mean erosion rate of 2.1 ± 1.2 cm yr^{-1} at the study site.

Table III. Characterization of root sections and erosion rates determined from wood anatomical changes

ID tree	ID of cross section	Geomorphic unit	Stratum	Ex (cm)	Age (years)	Year of exposure	NRex (years)	Erosion rate (root section scale, cm yr^{-1})	Erosion rate (root scale, cm yr^{-1})
1	1	Pb	2	5.2	18	2000	12	0.4	0.9
1	2	Pb	2	10.5	19	2000	12	0.875	
1	3	Pb	1	14.5	20	2000	12	1.2	
1	4	Pb	1	13	19	2000	12	1.08	
3	1	Rp	4	45	28	1996	16	2.81	2.7
3	2	Rp	3	50	28	1994	18	2.78	
3	3	Rp	2	62	26	1994	18	3.44	
3	4	Rp	2	60	28	1994	18	3.33	
3	5	Rp	1	60	26	1994	18	3.33	
3	6	Rp	1	55	28	1991	21	2.61	
3	7	Rp	1	34	29	1996	16	2.12	
3	8	Rp	1	18	29	1998	14	1.28	
4	1	Rp	3	27.5	15	2004	8	3.05	2.4
4	2	Rp	3	23	14	2005	7	3.28	
4	3	Rp	3	21	13	2003	9	2.33	
4	4	Rp	2	13.7	15	2004	8	1.71	
4	5	Rp	2	8.5	17	2006	6	1.41	
5	1	Rp	4	28	15	2004	8	3.5	3.9
5	2	Rp	4	34.5	14	2004	8	4.31	
5	3	Rp	4 (B)	−3	15				
5	4	Rp	4 (B)	−10	17				
5	5	Rp	4 (B)	−18	16				
6	1	Pb	3	6.5	22	2002	10	0.65	1.5
6	2	Pb	3	15	20	2002	10	1.5	
6	3	Pb	3	22.5	26	2002	10	2.25	
7	1	Pb	3	4.5	19	2002	10	0.45	0.6
7	2	Pb	3	4	19	2002	10	0.4	
7	3	Pb	3	9.5	19	2002	10	0.95	
8	1	Pb	3	5	23	2002	10	1.05	1.05
8	2	Pb	3	10.5	20	2002	10	1.05	
9	1	Pb	3	17.5	18	2005	7	2.5	1.9
9	2	Pb	3	6	18	2006	6	2.91	
9	3	Pb	3	12.5	19	2005	7	1.78	
9	4	Pb	3	12	19	2002	10	1.2	
9	5	Pb	3	12	18	2004	8	1.5	
10	1	Pb	2	15	22	2001	11	1.36	0.9
10	2	Pb	2	5	23	2001	11	0.45	
11	1	Pb	3	43	20	1996	16	2.68	1.7
11	2	Pb	2	10.5	19	1998	14	0.75	
12	1	Pb	3	50	28	1995	17	2.94	2.4
12	2	Pb	2	33.5	27	1995	17	1.97	
13	1	Pb	3	8	20	2001	11	0.72	0.6
13	2	Pb	3	4	20	2003	9	0.44	
14	1	Pb	2	2	15	2006	6	3.33	2.5
14	2	Pb	2	17.8	14	2006	6	2.96	
15	1	Pb	3	21	26	1997	15	1.4	1.6
15	2	Pb	3	21.5	28	2000	12	1.79	
16	1	Pb	4	87	35	1995	17	5.11	3.9
16	2	Pb	4	48	33	1998	14	3.42	
16	3	Pb	3	48	34	2000	12	4	
16	4	Pb	3	37.5	36	2000	12	3.125	
16	5	Pb	3 (B)	−2	32				
16	6	Pb	3 (B)	−8	33				
16	7	Pb	3 (B)	−13	37				
17	1	Pb	4	54	33	1997	15	3.6	3.3
17	2	Pb	3	36	27	2000	12	3	

Note: Pb = pocket beach; Rp = Rocky point; B = buried.

Variability of erosion rates

At the scale of individual roots, erosion rates varied between 0.6 (R7 and R13) and 3.9 cm yr^{-1} (R5 and R16, Table III). The largest erosion values were observed in roots (R3, R4, R5) sampled at Pointe de la Tufière located in the northeast (NE) part of the study site (Figure 4) and where the cliff is exposed directly to waves and storm surges. As a consequence, cliff retreat varies between 2.3 and 3.9 cm yr^{-1} here. Conversely, those roots sampled on cliffs backing La Courtade pocket beach (R1, R6–R10, R13, R15), sometimes protected by a vegetation buffer (R13, R15), recorded remarkably lower erosion rates ranging from 0.6 to 1.9 cm yr^{-1}.

At the root section scale, heterogeneous erosion rates are reconstructed for sections within the same root. For example, high variability between sections of the same root is observed in R11.

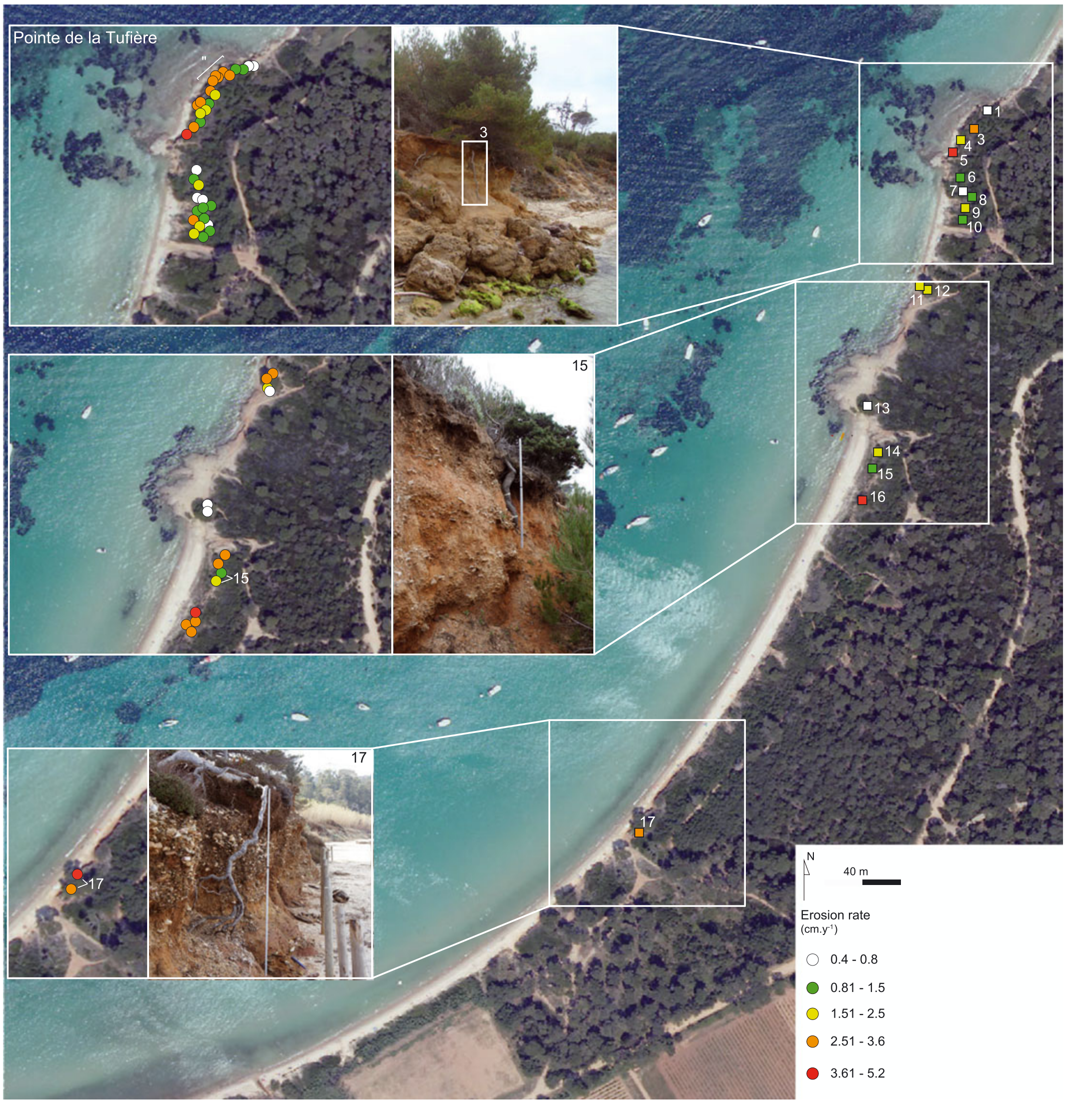

Figure 4. Cliff retreat map reconstructed from anatomical changes in exposed roots. Squares, on the right panels, represent mean erosion rates as computed for each of the 16 sampled roots. Dots, on the left panels, represent erosion rates as computed for each of the 50 sections. [Colour figure can be viewed at wileyonlinelibrary.com]

Here the ratio between the smallest and largest erosion rates is 1:3.6 (R11.2 in stratum 2 with 0.75 cm yr^{-1}; R11.1 in stratum 3 with 2.7 cm yr^{-1}). Similar differences are observed in R1 with a ratio of 1:3 between R1.1 (stratum 2, 0.4 cm yr^{-1}) and R1.3 (stratum 1, 1.2 cm yr^{-1}). According to the stratigraphic profile, highest erosion rates are reconstructed for root sections located in the upper part of the profile, i.e. in the sandy-gravelly stratum 4 (3.8 ± 0.8 cm yr^{-1}). Conversely, lower (1.8–2 cm yr^{-1}), but more variable, cliff retreat rates are measured in strata 1 (sandy stratum), 2, and 3 (torrential strata, Figure 5).

Reconstruction of cliff profiles

Dendrogeomorphic analyses do not only allow detection of root exposure processes with annual resolution, but also enable

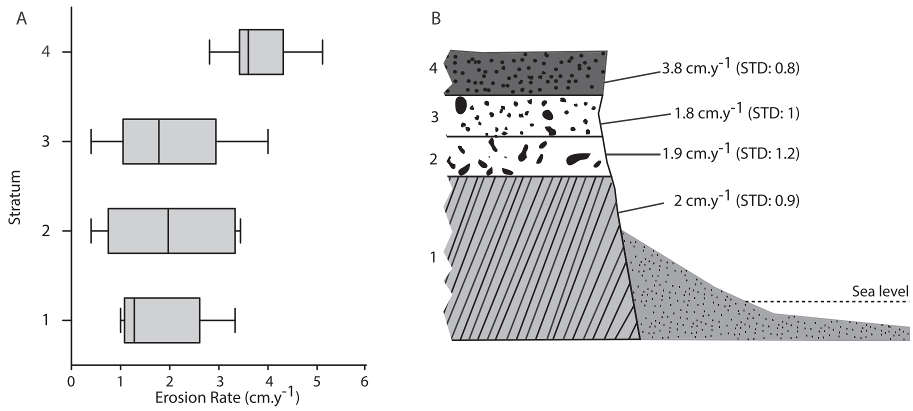

Figure 5. Comparison of cliff retreat for each stratum derived from anatomical changes in tree roots. 1. Sandy stratum, 2. Torrential deposits with decimetric debris, 3. Torrential deposit with centimetric debris, 4. Top sandy-gravelly stratum.

reconstruction of past cliff surface positions with centimetric precision. The use of exposed roots intersecting several strata therefore also allows the reconstruction of the spatio-temporal evolution of cliff profiles, as exemplified in Figure 6. The combined analysis of root positions and years of exposure thus provides a chronological framework to study cliff evolution and permits determination of erosion processes. By way of example, erosion at the level of root R3 occurred in three stages. The first stage corresponds to the first year of root exposure in 1991 at the level of sample R3.6, where anatomical changes can be observed in the cell structure of the root. This portion of the root was located in a top layer of fine sand (stratum 1). By contrast, no significant cell variations are observed in the other sections in that year. The second stage occurred in 1994 when anatomical changes start to occur in sections R3.2 to R3.5. This stage corresponds to a marked retreat in strata 1, 2, and 3, and is interpreted as the impact of a small landslide out of the notch in the weak sandy stratum. The third stage was initiated in 1996 and corresponds to a slow evolution of the top of the profile (stratum 4) as revealed by anatomical changes in R3.1 and to a delayed exposure of the foot cliff revealed by the exposure of R3.8 in 1998.

Discussion

Occurrence of anatomical changes in buried roots

In this study, we investigate the wood anatomical reaction of roots of *P. halepensis* Mill. to denudation and determine the timing of cliff retreat in the sandy-gravelly cliffs of Porquerolles Island. Anatomical reactions in roots have been used repeatedly to assess exposure dates, but never so far in a marine context. Recent work by Corona *et al.* (2011a, 2011b) in marly badlands of the southern French Alps demonstrated that changes in root cell anatomy and the related reduction of tracheid cell lumen area start to emerge as soon as the soil is reduced to about 3 cm, thus resulting in a bias of reconstructed sheet erosion. In order to ascertain for the existence of this bias in coastal cliffs, we based our analysis on a systematic and high resolution, quantitative assessment of changes in cell lumen area in exposed as well as buried roots sampled at various depths below the current cliff surface (Table III).

Results demonstrate that the reduction in cell lumen area of earlywood tracheids does not occur in buried sections of the root, thus confirming that the reduction in the earlywood tracheids lumen area corresponds exactly to the year at which the root section was exposed. At our study site, this absence of a bias can be explained by the milder climatic conditions of Porquerolles Island where frost is unusual. In the southern French Alps, by contrast, the triggering of anatomical changes in buried roots is attributed to freeze–thaw cycles that increase the vulnerability of the xylem to cavitation (Pittermann and Sperry, 2003). Also the results demonstrate that the abrupt cellular metamorphosis observed after exposure is induced by instantaneous erosion processes. Similarly, sharp reductions of the cell sizes in roots have been observed in *Fraxinus excelsior* L. root sections exposed along riverbanks in the Swiss Alps (Hitz *et al.*, 2008a). At the same time, values found in the present study clearly differ from the gradual evolution of cell lumen areas observed in the marly badlands of the southern French Alps (Corona *et al.*, 2011b). Such differences result from the nature of erosion processes involved in root exposure at each of the regions: i.e. continuous and regular erosion processes such as rill-wash in the badlands of Draix (Rovéra and Robert, 2005), and the sudden processes such as landslides or wall collapses at Porquerolles Island, or debris-flow events in the Swiss torrents.

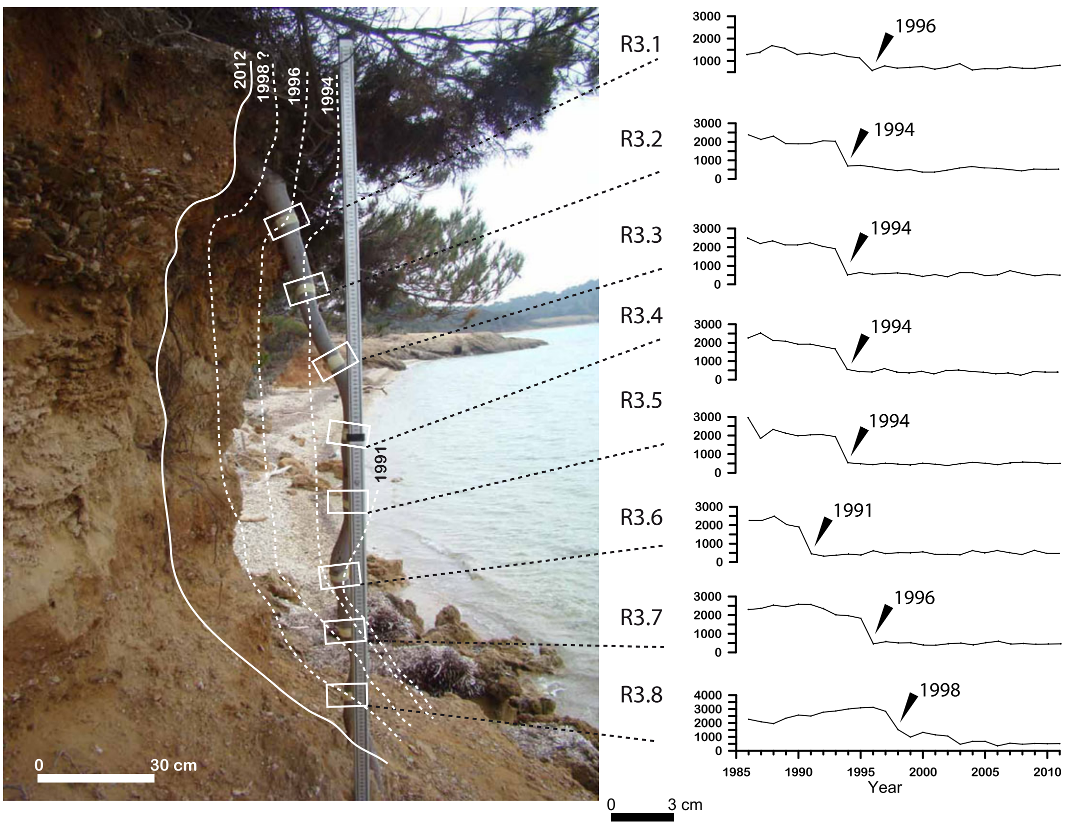

Figure 6. Evolution of cliff profiles since 1991 exemplified from root R3. Determination of exposure years was based on the sharp decrease of cell lumen area of earlywood tracheids. [Colour figure can be viewed at wileyonlinelibrary.com]

Reliability of erosion rates derived from dendrogeomorphic measurements

At Porquerolles, average erosion rates derived from root-ring analysis of *P. halepensis* Mill. are reaching rates up to 20 times higher than those calculated using tree roots in continental environments (soil erosion, bank erosion, and gully retreat) (Table II). Such discrepancies are probably related to the high sensitivity of the soft sandy-marly deposits to sudden erosion processes resulting from the mechanic impact of waves and swells at the foot of the cliffs. In detail, erosion rates are highest in the top (stratum 4) and basal (stratum 1) sandy strata (≥ 2 cm yr^{-1}). Similar results have been obtained at Carry-le-Rouet (Provence, France), where erosion rates three times higher in sandy-marly deposits than in calcarenite or conglomeratic deposits (Premaillon *et al.*, 2016), thus confirming that soft lithologies are more affected by erosion than indurated deposits (as also reported elsewhere by Moore and Griggs, 2002; Collins and Sitar, 2008; Lee, 2008; Young *et al.*, 2009b).

Erosion rates at our site vary between 0.6 and 3.9 cm yr^{-1}, with maxima observed on rocky points (at the root scale) and in stratum 4 (at the root section scale). By contrast the lowest retreat rates are reconstructed in those portions of the cliff protected by La Courtade pocket beach. These results are in line with Earlie *et al.* (2015a) who observed strong spatial variability (0.01–0.37 m yr^{-1}) in the recession rates of cliffs located on the south-western UK peninsula in relation with varying boundary conditions (i.e. rock mass characteristics, cliff geometries, beach morphology) and forcing parameters (i.e. significant wave height and peak wave period) (Earlie *et al.*, 2015b).

Quite interestingly, and despite their wide geographic extent over the Mediterranean region, only a very limited literature exists on rock coast recession, especially in soft rock lithologies (Earlie *et al.*, 2015b). Giuliano (2015), for instance, estimated erosion rates in Mediterranean sandy-gravelly cliffs of the Massif de la Nerthe (Carry-le-Rouet, France) through the comparison of (i) yearly-resolved LiDAR data with (ii) a multi-decadal, diachronic analysis of orthorectified aerial photographs covering the period 1924–2011. Cliff retreats derived from both methods are 1.1 cm yr^{-1} over a 17 month period and 4 ± 0.3 cm yr^{-1} over a 88-year period, respectively (Giuliano, 2015). These erosion rates are within the range of erosion rates reconstructed from exposed roots at Porquerolles Island (0.6–3.9 cm yr^{-1}). Our results are also comparable with cliff retreat rates (2–6 cm yr^{-1}) derived from diachronic analyses in the Calanque des Maures (France, Figure 1) on similar lithology (Giuliano, 2015). Apart from the methods used to derive erosion rates (i.e. photogrammetry, LiDAR and diachronic analysis versus root exposure), discrepancies between Porquerolles and Carry-le-Rouet may result from the different resolution of both studies. While Giuliano (2015) computed quasi-continuous cliff retreat rates for a 1-km long coastline at Carry-Le-Rouet, our study site is restricted to La Tufière headland and two locations points along one beach and does not exceed a total length of 150 m.

Noteworthy, and in a Mediterranean context (Figure 7, Table I) the cliff retreat rates derived from dendrogeomorphic reconstructions are much smaller than those measured in sandy-silty environments of Greece (50 cm yr^{-1}, Xeidakis *et al.*, 2007), in bio-calcarenites of Italy (20 cm yr^{-1}, Andriani and Walsh, 2007), and in the quartzose environments of Israel (20 cm yr^{-1}, Zviely and Klein, 2004) (Table I, Figure 7). At the hemispheric scale, by contrast, our results are in the same order of magnitude as erosion rates derived from 257

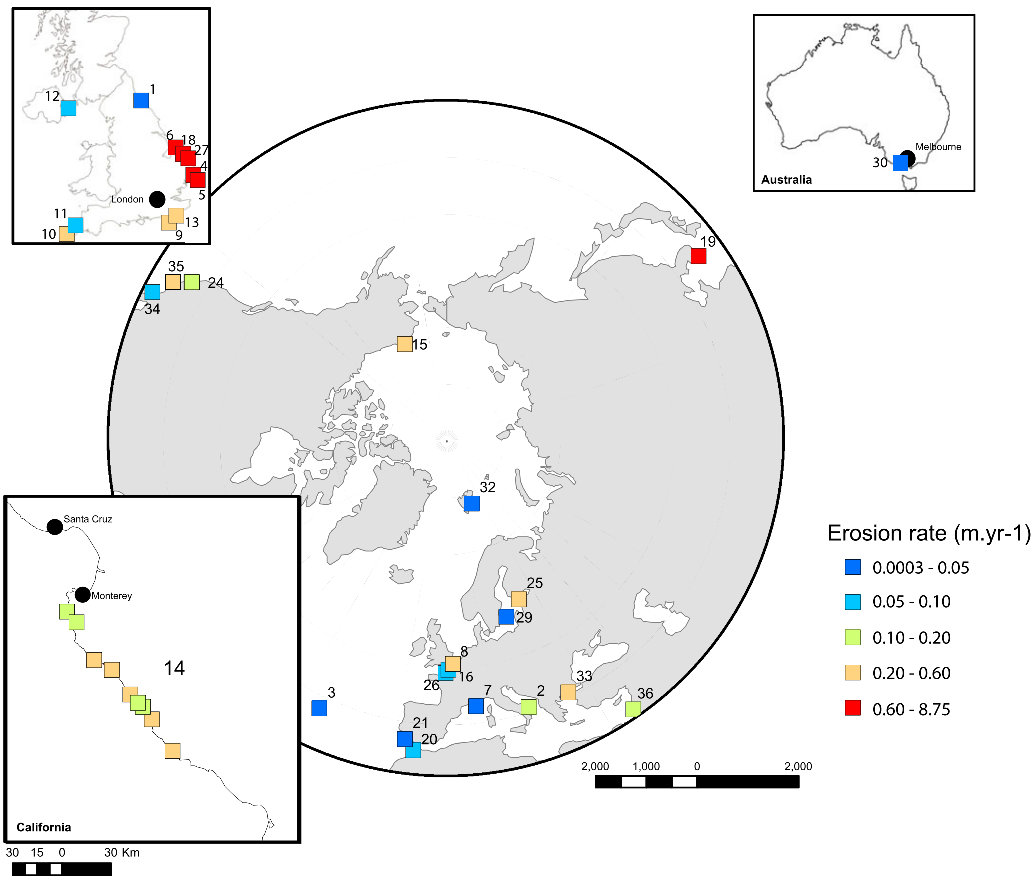

Figure 7. Map showing coastal cliff retreat rates obtained from the literature. Identifiers are the same as in Table I. [Colour figure can be viewed at wileyonlinelibrary.com]

Table IV. Advantages and limitations of common and root-based techniques to measure coastal cliff erosion (adapted from Trenhaile, 2011)

Technique	Advantages	Disadvantages
	Very accurate	Poor temporal and spatial coverage
Ground surveys	Easily repeatable	Time consuming (therefore expensive)
	Inexpensive	Low accuracy
	Widely available	Ambiguous cliff/bluff edge position
	Very long temporal coverage (since 1850s)	
Historical maps	Good spatial coverage	
	Inexpensive	Low accuracy
	Widely available	Ambiguous cliff/bluff position in two-dimensions
	Good temporal coverage (since 1920s)	
Aerial photographs unrectified	Good spatial coverage	
	Widely available	Ambiguous cliff/bluff position in two-dimensions
	Good temporal coverage (since 1920s)	Hardware/software for processing may be expensive
	Good spatial coverage	
Rectified partially	Improved accuracy over unrectified	
	Widely available	Processing time consuming
	Good temporal coverage (since 1920s)	Required software expensive
	Good spatial coverage	
	Very high accuracy	
Fully	Cliff/bluff edge can be digitized in 3D	
	Good spatial coverage	Expensive
	Very high accuracy	Poor temporal coverage
LiDAR		Cliff edge may not be captured in data
	Inexpensive	Presence/absence of trees
	Quantification of erosion rates in undocumented areas	Problem of non-homogeneous spatial distribution
	Multi-decadal, continuous reconstructions	Data on averaged rates
	Cover a large range of processes	Not available for intense processes
	Easy realization (excellent cost–benefit ratio)	Destructive sampling
	Method calibrated	Increased uncertainty with increasing timescale
	Intermediate time window (years, decades, centuries)	
Dendrogeomorphology (exposed root)	Quantification at the plot scale	

photogrammetric analyses on sandstone cliffs in the Algarve region (1.9 cm yr^{-1}, Marques, 1997), North Yorkshire (3 cm yr^{-1}, Agar, 1960) or the Larache region (Morocco, 8 cm yr^{-1}, Marques, 2003). Conversely, they are low compared to those available for California on sandstone and sand-claystone cliffs (15–30 cm yr^{-1}, Moore and Griggs, 2002; Young *et al.*, 2009b; Table I, Figure 7) and for macrotidal cliffs in northern Europe (10–50 cm yr^{-1}) (see e.g. Dewez *et al.*, 2007; Lim *et al.*, 2010; Dewez *et al.*, 2013; Letortu *et al.*, 2014; Michoud *et al.*, 2015).

However, even if the Mediterranean context is not prone to frequent and spectacular cliff collapse events like those of the chalk cliffs of northern Europe (e.g. Duperret *et al.*, 2002; Costa *et al.*, 2004; Regard *et al.*, 2012; Dewez *et al.*, 2013), acceptability of risk in the vicinity of cliffs is subjected to increasing residential, touristic, and economic pressures (Giuliano, 2015).

Contributions and limitations of the approach

The centimetric resolution of dendrogeomorphic reconstructions and the multi-decadal time windows typically covered by roots facilitate the comparison of averaged erosion rates with meteorological records. Dendrogeomorphic analyses also require less time to be accomplished and exhibit a much better cost–benefit ratio than most other techniques used to infer erosion (Table IV). The analysis of sequential aerial photography and satellite imagery, sometimes supplemented by historic maps, has remained the main method to reconstruct decadal-scale records of cliff recession (Table I). These sources cover roughly the same time windows (up to one century) as tree roots but at a much lower spatial resolution as a result of (i) shrinkage and stretching of the physical document over time, in addition to (ii) general issues of accuracy and precision associated with map production in the case of old maps (Snyder, 1987); as well as a result of (iii) the intervals between image acquisition, in the case of aerial surveys, that do not permit to detect overly slow or very rapid changes along rock coasts (Trenhaile, 2011). The dendrogeomorphic approach may be also considered as very complementary to the shorter time series obtained through repeat monitoring and on long-term erosion rates derived from radioisotopes (Regard *et al.*, 2012). Erosion pins, for example, have proven useful in changes caused by weathering effects, but remain limited spatially as the surface of surveyed plots rarely exceeds a few square meters and furthermore monitoring of the nail networks is most often limited to a few years (Lim *et al.*, 2005). Similarly, terrestrial LiDAR provides resources to study the spatial distribution of sea-cliff activity and erosional processes at sub-annual timescales (e.g. Lim *et al.*, 2005; Young *et al.*, 2009a; Lim *et al.*, 2010; Quinn *et al.*, 2010; Young *et al.*, 2011; Barlow *et al.*, 2012), but typically only over very short periods that does not exceed a few years. Similarly, terrestrial laser scanning (TLS) from the beach or shore platform can monitor changes in the cliff face, including the detachment of rock fragments of only a few centimeters in size up to large falls, slides, and flows (Rosser *et al.*, 2005) though facilitating high resolution three-dimensional (3D) mapping of sea cliff morphologies. Similarly, high precision measurements such as repeat drone surveys coupled with seismic and/or wave data or video surveillance, enable sea–cliff interactions to be captured (see e.g. Letortu *et al.*, 2018). Yet, such a quantitative characterization of sea–cliff activity remains a challenging task mainly due to the frequent sampling intervals required to capture such short duration, spatially heterogeneous and often non-linear natural phenomena (Katz and Mushkin, 2013). On larger timescales, typically in the range 100–10 000 years, the use of radionuclides (e.g. Regard *et al.*, 2012) provides important time-averaged constraints for the cumulative geomorphic effect of the suite of erosional processes that drive coastal cliff retreat, but possibly lacks the temporal resolution to identify causes and drivers of erosion. In all of the earlier examples, the replication of measurements and spatial resolution of results are often hampered by the cost of measurements and heavy instrumentation. On a spatial plan, our study refines future sampling protocols in the cliff context. Reconstructions will be more accurate if samples are acquired carefully every 10 cm on the same root. This first study also reveals that, in the case of cliffs, sub-horizontal root sections represent the most valuable specimens to establish mean erosion rates for a given stratum. In addition, vertical sections can be used as complementary data in order to reconstruct the evolution of the cliff profile. Documentation of such detailed patterns of annual cliff profile evolution will enable comparison of rates of geomorphic processes with hydrodynamic and climatic events that have affected the major study area over the past decades.

In summary, the main advantages of the dendrogeomorphic approach to quantify cliff retreat relate to (i) the quantification of cliff retreat in undocumented areas, (ii) with annual resolution. The approach is complementary of the shorter time series obtained with repeat monitoring or more coarsely resolved records obtained from aerial photographs or cosmogenic radionuclide as it enables (iii) to quantify cliff retreat rates with a centimetric resolution and to reconstruct the evolution of the cliff geometry, at the plot scale, for intermediate time window (up to one century) thus offering (iv) the possibility to infer micro-geomorphic and climatic controls on the timing of cliff retreat.

Conversely, the key limitation of root-based analyses of erosion is related to the presence of trees and shrubs in the study area and to the age of roots available for analysis. Dendrogeomorphic reconstructions of erosion rates are also limited to partly exposed, alive roots with growing tips still in the ground (Krause and Eckstein, 1993; Stoffel *et al*., 2013). Indeed, the water absorbing part – or terminal system – of the root needs to remain underground to work properly and to prevent the death of the root. It implies that an exposed part of a living root is older than the erosion process (Vandekerckhove *et al*., 2001; Hitz *et al*., 2008a). In addition, the method relies on a sufficient number of exposed trees and roots (two or three roots per tree, five to 10 trees) and data processing requires the destruction of samples. Furthermore, recent advances in vegetation-based reconstructions of erosion indicate that large exposed roots would underestimate the real values of the erosion rates (Haubrock *et al*., 2009; Bodoque *et al*., 2011; Stoffel *et al*., 2013). In a similar way, roots exposed over different periods in time and/or showing different ages may exhibit significant discrepancies in mean erosion rates. Finally, many of the ecosystems in regions with distinct seasons and the presence of trees are clearly dominated by broadleaved species (angiosperms). Despite their abundance, not least in areas affected by erosion, they have only rarely been used so far to reconstruct erosion processes, presumably as a result of their more complex wood anatomy and the existence of frequent growth anomalies (Cherubini *et al*., 2003). Some of the limitations of reconstructions with Mediterranean broadleaves have been illustrated by Bodoque *et al*. (2005). Roots of broadleaved trees growing in the more temperate climatic zones of Europe appear to be less affected by cambium stress and the formation of false or double rings and therefore have been used occasionally to infer erosion processes in the past (Malik, 2006; Hitz *et al*., 2008a, 2008b). Based on the earlier limitations and in an attempt to increase accuracy of reconstructions (while reducing the effect of biases), further calibration and validation of dendrogeomorphic results are needed on sites where erosion rates are monitored continuously and with high accuracy.

Conclusion

The analysis of anatomical changes in exposed tree roots for the quantification of erosion rates is fairly recent, and only starts to be applied to various geomorphic and geological contexts (refer to Stoffel *et al*. [2013] for a recent review). In the past, the approach was mainly used for the reconstruction of abrupt and severe erosion pulses resulting from gullying or torrential activity and for the quantitative analysis of continuous and areal erosion processes. In this study, we demonstrate that decadal erosion rates from exposed roots of *P. halepensis* Mill. can be used to infer the evolution of cliff profiles with high accuracy and precision in Quaternary sediments cliffs. Average erosion rates derived from root rings of Aleppo pine are highest on rocky points and at the top of sandy-gravelly strata of the slope profile. Results obtained with the dendrogeomorphic approach do not differ significantly from erosion rates from the literature obtained with more sophisticated and/or continuous measurements. The approach presented in this paper thus adds significantly to the methods available to understand sea cliff evolution and facilitates identification of areas of rapid erosion. The present study confirms the usefulness and importance of dendrogeomorphic approaches for the quantification of erosion in soft coastal rock environments, particularly for coastal areas where instrumental data are scarce or completely missing, and calls for more research in these environments.

Acknowledgements—This research has been supported by ANR CAPTIVEN (Capteurs et données pour la qualité environnementaledes eaux et des sols). The authors acknowledge the valuable input from anonymous referees and ESPL's editorial team.

References

Alestalo J. 1971. Dendrochronological interpretation of geomorphic processes. *Fennia* **105**(1).

Agar R. 1960. Post-glacial erosion of the north Yorkshire coast from the trees estuary to ravenscar. *Proceedings of the Yorkshire Geological Society*: 409–428.

Andriani GF, Walsh N. 2007. Rocky coast geomorphology and erosional processes: a case study along the murgia coastline south of Bari, Apulia — SE Italy. *Geomorphology* **87**: 224–238.

Arbellay E, Corona C, Stoffel M, Fonti P, Decaulne A. 2012. Defining an adequate sample of earlywood vessels to detect wound effects in diffuse-porous species. *PLoS ONE* **7**: e38824. https://doi.org/10.1371/journal.pone.0038824.

Bahrami S, Mahboobi F, Sadidi J, Aghdam MJ. 2011. Estimating the rate of sheet erosion by dendrogeomorphological analysis. *Physical Geography Research Quarterly* **43**: 1390.

Ballesteros-Cánovas JA, Bodoque JM, Lucía A, Martín-Duque JF, Díez-Herrero A, Ruiz-Villanueva V, Rubiales JM, Génova M. 2013. Dendrogeomorphology in badlands: methods, case studies and prospects. *Catena* **106**: 113–122.

Ballesteros-Cánovas JA, Corona C, Stoffel M, Lucia-Vela A, Bodoque JM, Martin-Duque JF. 2015. Combining terrestrial laser scanning and exposed roots for erosion rate estimation. *Plant and Soil* **394**: 127–137.

Ballesteros Cánovas JA, Stoffel M, Martín-Duque JF, Corona C, Lucía A, Bodoque JM, Montgomery DR. 2017. Gully evolution and geomorphic adjustments of badlands to reforestation. *Science Reports* **7**: 45027. https://doi.org/10.1038/srep45027.

Barlow J, Lim M, Rosser N, Petley D, Brain M, Norman E, Geer M. 2012. Modeling cliff erosion using negative power law scaling of rockfalls. *Geomorphology* **139–140**: 416–424. https://doi.org/10.1016/j.geomorph.2011.11.006.

Bellot JP. 2004. Mise en évidence d'un décrochement ductile senestre dans l'île de Porquerolles (Var, France) et ses implications sur la techtonique du Massif des Maures au Palézoïque. *Comptes Rendus Geoscience* **336**: 67–74. https://doi.org/10.1016/j.crte.2003.09.017.

Bodoque J, Ballesteros-Canovas J, Lucia A, Diez-Herrero A, Martin-Duque JF. 2015. Source of error and uncertainty in sheet erosion rates estimated from dendrogeomorphology. *Earth Surface Processes and Landforms* **40**(9): 1146–1157.

Bodoque J, Díez-Herrero A, Martín-Duque J, Rubiales J, Godfrey A, Pedraza J, Carrasco R, Sanz M. 2005. Sheet erosion rates determined by using dendrogeomorphological analysis of exposed tree roots: two examples from central Spain. *Catena* **64**: 81–102. https://doi.org/10.1016/j.catena.2005.08.002.

Bodoque J, Lucía A, Ballesteros J, Martín-Duque J, Rubiales JM, Genova M. 2011. Measuring medium-term sheet erosion in gullies from trees: a case study using dendrogeomorphological analysis of exposed pine roots in central Iberia. *Geomorphology* **134**: 417–425. https://doi.org/10.1016/j.geomorph.2011.07.016.

Bordet P, Blanc J, Jeudy de Grissac A, Chamley H, Durozoy G. 1976. *Hyères-Porquerolles, carte géologique de la France au 1:50.000.* Bureau de Recherches Géologiques et Minières (BRGM): Paris Vol. XXXIV, 21.383.

Borges P. 2003. *Ambientes litorais nos grupos Central e Oriental do arquipélago dos Açores, conteúdos e dinamîca de microescala*, PhD Thesis, University of the Azores (in Portuguese).

Brooks SM, Spencer T. 2010. Temporal and spatial variations in recession rates and sediment release from soft rock cliffs, Suffolk coast, UK. *Geomorphology* **124**(1–2): 26–41.

Brooks SM, Spencer T, Boreham S. 2012. Deriving mechanisms and thresholds for cliff retreat in soft-rock cliffs under changing climates: rapidly retreating cliffs of the Suffolk coast, UK. *Geomorphology* **153–154**: 48–60.

Brooks SM, Spencer T, McIvor A, Möller I. 2016. Reconstructing and understanding the impacts of storms and surges, southern North Sea. *Earth Surface Processes and Landforms* **41**(6): 855–864.

Carrara PE, Carroll TR. 1979. The determination of erosion rates from exposed tree roots in the Piceance Basin, Colorado. *Earth Surface Processes* **4**: 307–317.

Chartier MP, Giantomasi MA, Renison D, Roig FA. 2016. Exposed roots as indicators of geomorphic processes: A case-study from Polylepis mountain woodlands of Central Argentina. *Dendrochronologia* **37**: 57–63.

Chartier MP, Rostagno CM, Roig FA. 2009. Soil erosion rates in rangelands of north-eastern Patagonia: a dendrogeomorphological analysis using exposed shrub roots. *Geomorphology* **106**: 344–351.

Cherubini P, Gartner BL, Tognetti R, Bräker OU, Schoch W, Innes JL. 2003. Identification, measurement and interpretation of tree-rings inwoody species from mediterranean climates. *Biological Reviews of the Cambridge Philosophical Society* **78**: 119–148. https://doi.org/10.1017/S1464793102006000.

Collins B, Sitar N. 2008. Processes of coastal bluff erosion in weakly lithified sands, Pacifica, California, USA. *Geomorphology* **97**(3): 483–501. https://doi.org/10.1016/j.geomorph.2007.09.004.

Corona C, Lopez Saez J, Rovéra G, Astrade L, Stoffel M, Berger F. 2011a. Validation d'une méthode de quantification des vitesses d'érosion sur marnes par dendrogéomorphologie (draix, alpes de haute-provence). *Géomorphologie: relief, processus, environnement* (1): 83–94. https://doi.org/10.4000/geomorphologie.9254.

Corona C, Lopez Saez J, Rovéra G, Stoffel M, Astrade L, Berger F. 2011b. High resolution, quantitative reconstruction of erosion rates based on anatomical changes in exposed roots at Draix, Alpes de Haute-Provence — critical review of existing approaches and independent quality control of results. *Geomorphology* **125**: 433–444. https://doi.org/10.1016/j.geomorph.2010.10.030.

Costa S, Delahaye D, Freiré-Diaz S, Davidson R, Di Nocera L, Plessis E. 2004. Quantification of the Normandy and Picardy chalk cliff retreat by photogrammetric analysis. In *Coastal Chalk Cliff Instability*, Mortimore RN, Duperret A (eds). Engineering Geology, Special Publication 20. Geological Society: London; 139–148 https://doi.org/10.1144/GSL.ENG.2004.020.01.11.

Danzer SR. 1996. Rates of slope erosion determined from exposed roots of ponderosa pine at Rose Canyon Lake, Arizona. In *Tree Rings, Environment, and Humanity*, Dean J, Meko DM, Swetnam TW (eds). University of Arizona: Tucson, AZ; 671–678.

Dewez TJB, Rohmer J, Closset L. 2007. Laser survey and mechanical modelling of chalky sea cliff collapse in Normandy, France. In *Proceedings of the International Conference on Landslides and Climate Changes*, Ventnor, UK; 281–288.

Dewez TJB, Rohmer J, Regard V, Cnudde C. 2013. Probabilistic coastal cliff collapse hazard from repeated terrestrial laser surveys: case study from Mesnil Val (Normandy, northern France). *Journal of Coastal Research* **65**: 702–707. https://doi.org/10.2112/SI65-119.1.

Dick BM, Hey R, Peralta P, Jewell I, Simon P, Peszlen I. 2013. Estimating annual riverbank erosion rates–a dendrogeomorphic method. *River Research and Applications* **30**(7): 845–856.

Dornbusch U, Robinson DA, Moses CA, Williams RBG. 2008. Temporal and spatial variations of chalk cliff retreat in East Sussex, 1873 to 2001. *Marine Geology* **249**(3–4): 271–282.

Dunne T, Dietrich WE, Brunengo J. 1978. Recent and past erosion rates in semi-arid Kenya. *Zeitschrift für Geomorphologie* **29**: 130–140.

Duperret A, Genter A, Mortimore RN, Delacourt B, De Pomerai MR. 2002. Coastal rock cliff erosion by collapse at Puys, France: the role of impervious marl seams within chalk of NW Europe. *Journal of Coastal Research* **18**(1): 52–61.

Eardley A, Viavant W. 1967. *Rates of Denudation as Measured by Bristlecone Pines*, Special Studies, 21. Utah Geological and Mineralogical Survey: Cedar Breaks, UT; 13.

Earlie CS, Masselink G, Russell PE, Shail AK. 2015a. Application of airborne LiDAR to investigate rates of recession in rocky coast environments. *Journal of Coastal Conservation* **19**(6): 831–845. https://doi.org/10.1007/s11852-014-0340-1.

Earlie CS, Young AP, Masselink G, Russel PE. 2015b. Coastal cliff ground motions and response to extreme storm waves. *Geophysical Research Letters* **42**(3): 847–854.

Fantucci R. 2007. Dendrogeomorphological analysis of shore erosion along Bolsena lake (central Italy). *Dendrochronologia* **24**: 130–140. https://doi.org/10.1016/j.dendro.2006.11.002.

Gärtner H, Schweingruber FH, Dikau R. 2001. Determination of erosion rates by analyzing structural changes in the growth pattern of exposed roots. *Dendrochronologia* **19**: 81–91.

Gervais M. 2012. *Impacts morphologiques des surcotes et vagues de tempêtes sur le littoral méditerranéen*, PhD Thesis. University of Perpignan; 401.

Giuliano J. 2015. *Érosion des falaises de la région Provence-Alpes-Côte d'Azur: évolution et origine de la morphologie côtière en Méditerranée: télédétection, géochronologie, géomorphologie*, PhD Thesis. University of Nice Sophia Antipolis; 444 pp.

Granja HM. 2009. *Rocky Coasts in Coastal Zone and Estuaries*. UNESCO Encyclopedia of Life Support Systems (EOLSS): Paris; 540.

Greenwood RO, Orford JD. 2007. Factors Controlling the Retreat of Drumlin Coastal Cliffs in a Low Energy Marine Environment—Strangford Lough, Northern Ireland. *Journal of Coastal Research* **23**: 285–297. https://doi.org/10.2112/04-0417.1.

Hall JW, Meadowcroft IC, Lee EM, van Gelder PHAJM. 2002. Stochastic simulation of episodic soft coastal cliff recession. *Coastal Engineering* **46**: 159–174.

Hapke CJ, Green KR. 2004. *Map Showing Coastal Cliff Retreat Rates Along the Big Sur Coast (No. 2853).* Monterey and San Luis Obispo Counties: Monterey: CA.

Harper JR. 1978. Coastal erosion rates along the Chukchi Sea coast near Barrow, Alaska. *Arctic* **31**: 428–433.

Haubrock SN, Kuhnert M, Chabrillat S, Güntner A, Kaufmann H. 2009. Spatiotemporal variations of soil surface roughness from *in-situ* laser scanning. *Catena* **79**: 128–139. https://doi.org/10.1016/j.catena.2009.06.005.

Hénaff A, Lageat Y, Costa S, Plessis E. 2002. Le recul des falaises crayeuses du Pays de Caux: détermination des processus d'érosion et quantification des rythmes d'évolution. *Géomorphologie: relief, processus, environnement* **8**: 107–118.

Hitz O, Gärtner H, Heinrich I, Monbaron M. 2008a. Application of ash (*Fraxinus excelsior* l.) roots to determine erosion rates in mountain torrents. *Catena* **72**: 248–258. https://doi.org/10.1016/j.catena.2007.05.008.

Hitz O, Gärtner H, Heinrich I, Monbaron M. 2008b. Wood anatomical changes in roots of European ash (*Fraxinus excelsior* l.) after exposure. *Dendrochronologia* **25**: 145–152. https://doi.org/10.1016/j.dendro.2007.03.005.

Hurst MD, Rood DH, Ellis MA, Anderson RS, Dornbusch U. 2016. Recent acceleration in coastal cliff retreat rates on the south coast of Great Britain. *PNAS* **113**(47): 13336–13341.

Katz O, Mushkin A. 2013. Characteristics of sea-cliff erosion induced by a strong winter storm in the eastern Mediterranean. *Quaternary Research* **80**: 20–32. https://doi.org/10.1016/j.yqres.2013.04.004.

Kennedy M. 2009. *Introducing Geographic Information Systems with ARCGIS: A Workbook Approach to Learning GIS*. John Wiley & Sons: Hoboken, NJ; 672.

Krause C, Eckstein D. 1993. Dendrochronology of roots. *Dendrochronologia* **11**: 9–23.

Kumar A, Seralathan P, Jayappa KS. 2009. Distribution of coastal cliffs in Kerala, India: their mechanisms of failure and related human engineering response. *Environmental Geology* **58**(4): 815.

LaMarche VC. 1968. Rates of Slope Degradation as Determined from Botanical Evidence White Mountains California, United States Geological Survey Professional Paper 352-I. US Geological Survey: Reston, VA.

Lim DI, Choi JY, Jung HS. 2009. Sea-cliff erosion and retreat in semi-enclosed macrotidal embayment: Hampyung Bay, West coast of Korea. *Journal of Coastal Research (Proceedings of the 10th International Coastal Symposium, Lisbon, Portugal)* **56**(special issue): 732–736.

Lim M, Petley DN, Rosser NJ, Allison RJ, Long AJ, Pybus D. 2005. Combined digital photogrammetry and time-of-flight laser scanning for monitoring cliff evolution. *The Photogrammetric Record* **20**: 109–129. https://doi.org/10.1111/j.1477-9730.2005.00315.x.

Lim M, Rosser NJ, Allison RJ, Petley DN. 2010. Erosional processes in the hard rock coastal cliffs at Staithes, North Yorkshire. *Geomorphology* **114**: 12–21. https://doi.org/10.1016/j.geomorph.2009.02.011.

Lee EM. 2008. Coastal cliff behaviour: observations on the relationship between beach levels and recession rates. *Geomorphology* **101**: 558–571. https://doi.org/10.1016/j.geomorph.2008.02.010.

Letortu P, Costa S, Bensaid A, Cador JM, Quénol H. 2014. Vitesses et rythmes de recul des falaises crayeuses de Haute-Normandie (France): Méthodologie et variabilité du recul. *Géomorphologie, relief, processus et environnement* (2): 133–144.

Letortu P, Jaud M, Grandjean P, Ammann J, Costa S, Maquaire O, Davidson R, Le Dantec N, Delacourt C. 2018. Examining high-resolution survey methods for monitoring cliff erosion at an operational scale. *GIScience and Remote Sensing* **55**(4): 457–476. https://doi.org/10.1080/15481603.2017.1408931.

Lopez Saez J, Corona C, Stoffel M, Rovéra G, Astrade L, Berger F. 2011. Mapping of erosion rates in marly badlands based on a coupling of anatomical changes in exposed roots with slope maps derived from LiDAR data. *Earth Surface Processes and Landforms* **36**: 1162–1171. https://doi.org/10.1002/esp.2141.

Lucía A, Laronne JB, Martín-Duque JF. 2011. Geodynamic processes on sandy slope gullies in central Spain field observations, methods and measurements in a singular system. *Geodinamica Acta* **24**: 61–79.

Luo M, Zhou Y, Wang KK. 2011. Response of anatomical features of broadleaf tree root in Karst area to soil erosion. *Second SREE Conference on Chemical Engineering Book Series*, 18.

Malik I. 2006. Gully erosion dating by means of anatomical changes in exposed roots (Proboszczowicka plateau, southern Poland). *Geochronometria* **25**: 57–66.

Malik I. 2008. Dating of small gully formation and establishing erosion rates in old gullies under forest by means of anatomical changes in exposed tree roots (southern Poland). *Geomorphology* **93**: 421–436. https://doi.org/10.1016/j.geomorph.2007.03.007.

Malik I, Matyja M. 2008. Bank erosion history of a mountain stream determined by means of anatomical changes in exposed tree roots over the last 100 years. *Geomorphology* **98**: 126–142.

Marques F. 1997. *As arribas do litoral do algarve. dinamica, processos e mecanismos*, PhD Thesis. University of Lisbon, 556 pp.

Marques F. 2003. Landslide activity in upper palaeozoic shale sea cliffs: a case study along the western coast of the Algarve (Portugal). *Bulletin of Engineering Geology and the Environment* **62**: 299–313.

Martens DM. 1993. Hydrologic inferences from tree-ring studies on the Hawkesbury River, Sydney, Australia. *Geomorphology* **8**: 147–164. https://doi.org/10.1016/0169-555X(93)90034-Y.

McAuliffe JR, Scuderi LA, McFadden LD. 2006. Tree-ring record of hillslope erosion and valley floor dynamics: landscape responses to climate variation during the last 400yr in the Colorado plateau, northeastern Arizona. *Global and Planetary Change* **50**: 184–201. https://doi.org/10.1016/j.gloplacha.2005.12.003.

Megahan WF, Seyedbagheri KA, Dodson PC. 1983. Long-term erosion on granitic roadcuts based on exposed tree roots. *Earth Surface Processes* **8**: 19–28.

Mei L, Yunchao Z, Keke W. 2015. Soil erosion characteristics according to tree-rings in a karst area. *Journal of Ressources and Ecology* **6**(4): 257–262.

Michoud C, Carrea D, Costa S, Derron M-H, Jaboyedoff M, Delacourt C, Maquaire O, Letortu P, Davidson R. 2015. Landslide detection and monitoring capability of boat-based mobile laser scanning along Dieppe coastal cliffs, Normandy. *Landslides* **12**: 403–418.

Moon V, Healy T. 1994. Mechanisms of coastal cliff retreat and hazard zone delineation in soft flysch deposits. *Journal of Coastal Research* **10**: 663–680.

Moore LJ, Griggs GB. 2002. Long-term cliff retreat and erosion hotspots along the central shores of the Monterey bay national marine sanctuary. *Marine Geology* **181**: 265–283. https://doi.org/10.1016/S0025-3227(01)00271-7.

Nakamura F, Maita H, Araya T. 1995. Sediment routing analyses based on chronological changes in hillslope and riverbed morphologies. *Earth Surface Processes and Landforms* **20**(4): 333–346. https://doi.org/10.1002/esp.3290200404.

Naylor LA, Spencer T, Lane SN, Darby SE, Magilligan FJ, Macklin MG, Möller I. 2017. Stormy geomorphology: geomorphic contributions in an age of climate extremes. *Earth Surface Processes and Landforms* **42**: 166–190.

Orviku K, Tõnisson H, Kont A, Suuroja S, Anderson A. 2013. Retreat rate of cliffs and scarps with different geological properties in various locations along the Estonian coast. *Journal of Coastal Research* **65**: 552–557.

Pelfini M, Santilli M. 2006. Dendrogeomorphological analyses on exposed roots along two mountain hiking trails in the Central Italian Alps. *Geografiska Annaler* **88A**: 223–236.

Pérez-Rodríguez R, Marques MJ, Bienes R. 2007. Use of dendrochronological method in Pinus halepensis to estimate the soil erosion in the south east of Madrid (Spain). *Science of the Total Environment* **378**: 156–160.

Pierre G. 2006. Processes and rate of retreat of the clay and sandstone sea cliffs of the northern Boulonnais (France). *Geomorphology* **73**: 64–77.

Pittermann J, Sperry J. 2003. Tracheid diameter is the key trait determining the extent of freezing-induced embolism in conifers. *Tree Physiology* **23**(13): 907–914.

Poulton CVL, Lee JR, Hobbs PRN, Jones L, Hall M. 2006. Preliminary investigation into monitoring coastal erosion using terrestrial laser scanning: case study at Happisburgh, Norfolk. *The Bulletin of the Geological Society Norfolk* **56**: 45–64.

Premaillon M, Dewez TJB, Giuliano J, Marcot N. 2016. Repeated boatborne lidar survey to quantify coastal erosion in Carry-le-Rouet (southern France). *Virtual Geoscience Conference 2016*, Bergen, Norway, 21–23 September.

Quinn J, Rosser N, Murphy W, Lawrence J. 2010. Identifying the behavioural characteristics of clay cliffs using intensive monitoring and geotechnical numerical modelling. *Geomorphology* **120**: 107–122. https://doi.org/10.1016/j.geomorph.2010.03.004.

Regard V, Dewez T, Bourlès D, Anderson R, Duperret A, Costa S, Leanni L, Lasseur E, Pedoja K, Maillet G. 2012. Late Holocene seacliff retreat recorded by ^{10}Be profiles across a coastal platform: theory and example from the English Channel. *Quaternary Geochronology* **11**: 87–97. https://doi.org/10.1016/j.quageo.2012.02.027.

Rinn F, Jäkel S. 1996. *TSAP-reference manual*. Frank Rinn: Heidelberg; 262.

Rosser N, Petley D, Lim M, Dunning S, Allison R. 2005. Terrestrial laser scanning for monitoring the process of hard rock coastal cliff erosion. *Quarterly Journal of Engineering Geology and Hydrogeology* **38**(4): 363–375. https://doi.org/10.1144/1470-9236/05-008.

Rovéra G, Robert Y. 2005. Conditions climatiques hivernales et processus d'érosion périglaciaires dans les bad-lands marneux de Draix (800 m, Alpes du Sud, France). *Géographie Physique et Quaternaire* **59**: 31–48. https://doi.org/10.7202/013735ar.

Rubiales JM, Bodoque JM, Ballesteros JA, Diez-Herrero A. 2008. Response of *Pinussylvestris*roots to sheet-erosion exposure: an anatomical approach. *Natural Hazards and Earth System Sciences* **8**: 223–231. https://doi.org/10.5194/nhess-8-223-2008.

Rudberg S. 1967. The cliff coast of Gotland and the rate of cliff retreat. *Geografiska Annaler. Series A, Physical Geography* **49**: 283–298.

Schweingruber FH. 1978. *Microscopic Wood Anatomy*. Swiss Federal Institute of Forestry Research: Zurich.

Scuderi LA, McFadden LD, McAuliffe JR. 2008. Dendrogeomorphically derived slope response to decadal and centennial scale climate variability: Black Mesa, Arizona, USA. *Natural Hazards and Earth System Sciences* **8**: 869–880.

Silhan K. 2012. Dendrogeomorphological analysis of the evolution of slope processes on Flysch rocks (Vsetinske Vrchy Mts, Czech Republic). *Carpathian Journal of Earth and Environmental Sciences* **7**: 39–49.

Snyder J. 1987. *Map Projections – A Working Manual*, US Geological Survey Professional Paper 1395. US Geological Survey: Reston, VA.

Small C, Nicholls RJ. 2003. A global analysis of human settlement in coastal zones. *Journal of Coastal Research* **19**: 584–599.

Stephenson WJ, Kirk RM, Kennedy DM, Finlayson BL, Chen Z. 2012. Long term shore platform surface lowering rates: revisiting Gill and Lang after 32 years. *Marine Geology* **299–302**: 90–95.

Stoffel M, Bollschweiler M. 2008. Tree-ring analysis in natural hazards research – an overview. *Natural Hazards and Earth System Sciences* **8455**: 187–202.

Stoffel M, Bollschweiler M, Butler DR, Luckman B. 2010. *Tree Rings and Natural Hazards*. Springer: Dordrecht; 457 https://doi.org/10.1007/978-90-481-8736-2_1.

Stoffel M, Casteller A, Luckman BH, Villalba R. 2012. Spatiotemporal analysis of channel wall erosion in ephemeral torrents using tree roots – an example from the Patagonian Andes. *Geology* **40**: 247–250. https://doi.org/10.1130/G32751.1.

Stoffel M, Corona C, Ballesteros-Cánovas JA, Bodoque JM. 2013. Dating and quantification of erosion processes based on exposed roots. *Earth-Science Reviews* **123**: 18–34. https://doi.org/10.1016/j.earscirev.2013.04.002.

Stoffel M, Corona C. 2014. Dendroecological dating of geomorphic disturbance in trees. *Tree Ring Research* **70**: 3–20. https://doi.org/10.3959/1536-1098-70.1.3.

Stokes A, Berthier S. 2000. Irregular heartwood formation in *Pinuspinaster*Ait. is related to eccentric, radial, stem growth. *Forest Ecology and Management* **135**: 115–121. https://doi.org/10.1016/S0378-1127(00)00303-0.

Stotts S, O'Neal M, Pizzuto J, Hupp C. 2014. Exposed tree root analysis as a dendrogeomorphic approach to estimating bank retreat at the South River, Virginia. *Geomorphology* **223**: 10–18.

Strunk H. 1989. Dendrogeomorphology of debris flows. *Dendrochronologia* **7**: 15–25.

Strunk H. 1991. Frequency distribution of debris flow in the Alps since the "Little Ice Age". *Zeitschrift für Geomorphologie* **83**: 71–81.

Strunk H. 1997. Dating of geomorphological processes using dendrogeomorphological methods. *Catena* **31**: 137–151. https://doi.org/10.1016/S0341-8162(97)00031-3.

Sun L, Xiaodan W, Hong J. 2014. Response of anatomical structures in the tree roots to an erosion event on the southeastern Tibetan Plateau. *Geomorphology* **204**: 617–624.

Sunamura T. 1992. *Geomorphology of rocky coasts (Volume 3)*. John Wiley & Son: Chichester.

Trenhaile A. 2011. Cliffs and rock coasts. In *Treatise on Estuarine and Coastal Science*. Elsevier: Amsterdam; 171–191.

Trenhaile A. 2014. Climate change and its impact on rock coasts. In *Rock Coast Geomorphology: A Global Synthesis*, Kennedy DM, Stephenson WJ, Naylor LA (eds), Vol. **40**. Geological Society: London; Memoirs; 7–17.

Vandekerckhove L. 2001. Short-term bank gully retreat rates in Mediterranean environments. *Catena* **44**: 133–161. https://doi.org/10.1016/S0341-8162(00)00152-1.

Wangensteen B, Eiken T, Odegard RS, Sollid JL. 2007. Measuring coastal cliff retreat in the Kongsfjorden area, Svalbard, using terrestrial photogrammetry. *Polar Research* **26**: 14–21.

Watson A. 2000. Wind-induced forces in the near-surface lateral roots of Radiata pine. *Forest Ecology and Management* **135**: 133–142. https://doi.org/10.1016/S0378-1127(00)00305-4.

Wawrzyniec TF, McFadden LD, Ellwein A, Meyer G, Scuderi L, McAuliffe J, Fawcett P. 2007. Chronotopographic analysis directly from point-cloud data: a method for detecting small, seasonal hillslope change, Black Mesa Escarpment, NE Arizona. *Geosphere* **3**: 550–567.

Xeidakis GS, Delimani P, Skias S. 2007. Erosion problems in Alexandroupolis coastline, north-eastern Greece. *Environmental Geology* **53**: 835–848.

Young AP, Ashford SA. 2006. Application of airborne LiDAR for seacliff volumetric change and beach-sediment budget contributions. *Journal of Coastal Research* **22**: 307–318.

Young AP, Flick R, Gutierrez R, Guza R. 2009a. Comparison of short-term seacliff retreat measurement methods in Del Mar, California. *Geomorphology* **112**: 318–323. https://doi.org/10.1016/j.geomorph.2009.06.018.

Young AP, Guza R, Flick R, O'Reilly W, Gutierrez R. 2009b. Rain, waves, and short-term evolution of composite seacliffs in southern California. *Marine Geology* **267**: 1–7. https://doi.org/10.1016/j.margeo.2009.08.008.

Young AP, Guza RT, O'Reilly WC, Flick RE, Gutierrez R. 2011. Short-term retreat statistics of a slowly eroding coastal cliff. *Natural Hazards and Earth System Sciences* **11**: 205–217. https://doi.org/10.5194/nhess-11-205-2011.

Zhang K, Douglas BC, Leatherman SP. 2004. Global warming and coastal erosion. *Climatic Change* **64**: 41–58. https://doi.org/10.1023/B:CLIM.0000024690.32682.48.

Zhou F, Gou X, Zhang L, Cao Z, Zhao Z. 2013. Application of *Picea wilsonii* roots to determine erosion rates in eastern Qilian Mountains, northwestern China. *Trees – Structure and Function* **27**: 371–378.

Zviely D, Klein M. 2004. Coastal cliff retreat rates at Beit-Yannay, Israel, in the 20th century. *Earth Surface Processes and Landforms* **29**: 175–184.

